Article

Optimization and Performance Evaluation of a Foam Plugging Profile Control Well Selection System

Khwaja Naweed Seddiqi,* Kazunori Abe, Hongda Hao,* Zabihullah Mahdi, Huaizhu Liu, and Jirui Hou*

ACCESS | Metrics & More | Article Recommendations

ABSTRACT: Most of the oilfields are currently experiencing intermediate to late stages of oil recovery by waterflooding. Channels were created between the wells by water injection and its effect on the oil recovery is less. The use of water plugging profile control is required to control excessive water production from an oil reservoir. First, the well selection for profile control using the fuzzy evaluation method (FEM) and improvement by random forest (RF) classification model is investigated. To identify wells for profile control operation, a fuzzy model with four factors is established; then, a machine learning RF algorithm was applied to create the factor weight with high accuracy decision-making. The data source consists of 18 injection wells, with 70% of the well data being utilized for training and 30% for model testing. Following the fitting of the model, the new factor weight is determined and decisions are made. As a consequence, FEM selects 7 out of 18 wells for profile control, and by using the factor weight developed by RF, 4 out of 18 wells are chosen. Then, the profile control is conducted through a foam system proposed by laboratory experiments. A computer molding group numerical simulation model is created to profile the wells being selected by both methods, FEM and RF. The impact of foam system plugging on daily oil production, water cut, and cumulative oil production of both methods are contrasted. According to the study, the reservoir performed better when four wells were chosen by the weighting system developed by RF as opposed to seven wells that were chosen using the FEM model during the effective period. The weighting model developed by RF accurately increased the profile control wells' decision-making skills.
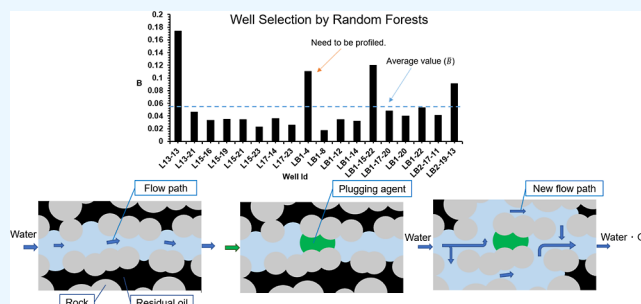
1. INTRODUCTION

Oil is one of the biggest energy resources for world consumption; it can be used in so many different ways, such as a material for public and private use. The conservation of crude oil reserves in countries is one of the most critical aspects in the macro-economic sphere and energy sectors of the countries. Through a reservoir management strategy, the development of the reservoirs' profit, enhancement of their recovery factor, and the final reduction of production costs are possible.[1] The normal production rate of oil is reducing day by day, and most of the big oil reservoirs in the world are in the second phase of their production stages.[2,3] Therefore, to maintain the production capacity of oil reservoirs, enhanced oil recovery techniques may be possible future solutions in the oil production industry.

It is overly simplistic to judge whether an oil well needs to be profile controlled by an oilfield site based on the water cut or simply based on experience. When numerous oil wells at the same time produce water, not every injection well needs to be plugged due to the various reasons for the water discharge. As a result, systematic well selection for profile control is required. The conventional approach of randomly choosing oil wells based on experience might occasionally exacerbate and

deteriorate the water production of additional oil wells around the block. Therefore, it is crucial to create a straightforward and accurate profile control well-selection system.[4−6]

To identify wells for profile control, two main ways are used. The first method of well selection is from a qualitative study,[7] while the second one is selected through the existing software packages. In the oil production industry, the fuzzy mathematic evaluation method is usually used to select the wells for profile control.[8−10] In the fuzzy evaluation method (FEM), the factor weight calculation is the key component of this method.[11] Liu et al. used RS software to optimize well efficiency by adjusting their water shut off and profile control procedures. The researchers combined numerical modeling and reservoir engineering to create an efficient method for optimizing wells.[11] A fuzzy clustering method is used by Jiang et al.[12] for

data collection and decision-making related to the well selection. It can help identify similarities among different wells by considering their various characteristics. The fuzzy clustering concept is a technique of data collection that is used for early warning well selection. It involves identifying similarities among different wells based on their water cut stage. Xia et al.[6] suggested a clustering algorithm that may be employed for candid well selection for profile control in a real oilfield. The weighting computation carried out by Li[13−15] is implemented by solving the matrix theory in the FEM. The decision-making technique for profile control well selection by using pressure index (PI) was developed by Wang et al.[16,17] This involves analyzing the wellbore problem and offering a strategy to select the right candidates.[18]

This paper presents FEM to select well candidates for profile control. The FEM finds the appropriate wells that can be used for profile control but the difficulty in calculating the weights of the various factors involved in the calculation makes the process challenging. In this method, the evaluation set has been made to enable the decision-makers to reach a well-selection result. A subjective weight system is commonly used in this method as it allows the participants to determine the weight for each factor. The weight can be critical in this method, so the results of this technique by using not accurate weight system are possibly inaccurate.

To improve the perfection of a well-selection decision, the factor weight calculation by random forest (RF) algorithm is used. The RF algorithm can calculate the factor weight with high accuracy based on the features that are considered in the FEM. Factor weight calculation and usage in FEM purposed by author, Seddiqi et al.[19] for the selection of production wells candidate for water shutoff is being used in this study.

In the next part, the performance and efficiency of the foam system for profile control are evaluated by laboratory experiments. A core flood test was prepared to study the foam plugging rate in reservoir conditions. Based on the core flood test and foam experiment, a computer molding group (CMG)-STARS numerical simulation model was created to evaluate and match the foam plugging simulation model with the laboratory experiment result.

The paper's final section includes a numerical simulation analysis to authenticate the new method applied for profile control. The numerical simulation study results are compared to those derived from three simulated models: a model with no wells selected for profile control; seven wells selected for profile control based on the FEM model; and four wells selected using the factor weight developed by the RF model and the production process is conducted from 2020 until 2025. Finally, the proposed methods in this research are compared with the well selection method by entropy offered in 2009 by Zheng and Tian.[20]

2. MATERIALS AND METHODS

2.1. FEM for Profile Control. *2.1.1. Establishing of Decision Factors for Profile Control Well Selection.* In the FEM, four factors, water absorption factor (K_h), apparent water absorption factor (K_s), pressure value of water injection well (PI), and permeability variation coefficient (K_v) can be applied to profile control selection to a certain extent. However, since these factors are all qualitative factors, they cause inconvenience in well-selection calculations. These factors are transformed into quantitative factors, and those

qualitative factors are selected using quantitative concepts, and then, profile control and well selection are performed.

Therefore, the uncertainty method of expert knowledge is used to normalize the factor parameters, introduce the membership degree to indicate the importance of each factor's determining factor, and use the trapezoidal distribution to select the membership function. The larger the value of the three factors K_h, K_s, and K_v, the more the corresponding water injection well needs profile control. Therefore, the ascending semi-trapezoidal distribution expresses the three factors mentioned above. The larger the PI value, the less profile adjustment is needed for the well, so a half-trapezoidal distribution is adopted for it.

(1) Water absorption index (K_h). K_h is equal to the water injection volume (m^3/d) of the oil layer under the unit production pressure difference.

$$K_h = \frac{Q}{(P_{wf} - P_e)h} \tag{1}$$

In the formula, K_h is the index of water absorption, $m^3/(d \cdot MPa \cdot m)$; Q is the water injection volume of the water injection well, m^3/d; P_{wf} is the water injection wells' bottom hole pressure, MPa; P_e is the oil layer of the water injection well Static pressure, MPa; and h is the water-absorbing oil layer's thickness, m.

In practical applications, the K_h can be calculated from the water injection well water absorption indicator curve.

$$K_h = \frac{Q_2 - Q_1}{(P_2 - P_1)h} \tag{2}$$

In eq 2, Q_1 and Q_2 are the volumes of daily water injection under two different working systems, m^3/d; P_1 and P_2 are the bottom hole flowing pressure under the corresponding two working systems, MPa.

(2) Apparent water absorption index (K_s). K_s is the daily water absorption per meter of the oil layer at a pressure of 1 MPa. For general water injection wells

$$K_s = \frac{Q}{P_w \cdot h} \tag{3}$$

In eq 3, K_s is the apparent water absorption index, $m^3/(d \cdot MPa \cdot m)$; Q is the volume of daily water injection, m^3/d; P_w is the injection pressure, MPa; and h is the thickness of water-absorbing oil layer, m. P_w is equal to wellhead casing pressure if water is injected from tubing, and P_w is equal to the wellhead oil pressure if water is injected from the casing. For the stratified injection wells

$$K_s = \frac{Q_i}{(P_w - \Delta P_i) \cdot h} \tag{4}$$

In eq 3, P_i is the wellhead pressure of the stratified water injection well, MPa; Q_i is the injection rate, m^3/d; and h is the thickness of the water-absorbing layer, m.

(3) PI value of the water injection well (PI). According to the actual measured pressure drop curve after the shut-in of the water injection well (assuming that the shut-in time is 90 min), the ratio of integral to time within a certain time interval is the PI value. The definition of the PI value is as follows.

$$PI = \frac{\int_0^t P(t)dt}{t} \quad (5)$$

In the formula, PI is the PI of the injection well, MPa; $p(t)$ is the wellhead oil pressure after the shut-in time of the water injection well, MPa; and t is the shut-in time, min. The following equation can also be used to determine the PI value when the physical characteristics of the reservoir block are known.

$$PI = \frac{q\mu}{15kh} \ln \frac{12.5r_e^2 \varphi \mu c}{kt} \quad (6)$$

In eq 6, q is the daily water injection, m^3/d; μ is the hydrodynamic viscosity, mPa·s; η is the pressure conduction coefficient, m^2/s; h is the formation thickness, m; k is the formation permeability, μm^2; t is shut-in test time, s; φ is the porosity, %; r_w is the radius of the wellbore, m; r_e is the radius of the injection well, m; and c is the comprehensive compressibility, Pa^{-1}.

The daily injection volume and oil layer thickness of different water wells are different. To put the PI values of different water injection wells in the same block together for sequence comparison, the PI values must be corrected to the same fluid injection intensity (daily injection volume and formation thickness ratio).

(4) Permeability variation coefficient (K_v). If the oil layer is heterogeneous and the thickness and permeability of each layer are different, the permeability variation coefficient K_v needs to be introduced to characterize the heterogeneity of the oil layer. K_v is calculated using the following formula.

$$K_v = \frac{\sqrt{\sum_{i=1}^n [(k_i - k)^2 \cdot h_i]}}{\sqrt{\sum_{i=1}^n h_i} \cdot k} \quad (7)$$

where k_i is the permeability of the i-th layer, μm^2; h_i is the thickness of the i-th layer, m; n is the layers' number; and k is the average permeability of all layers, μm^2.

$$k = \frac{\sum_{i=1}^n k_i \cdot h_i}{H} \quad (8)$$

H is the total thickness of each layer, m.

2.1.2. Creating a Weight Set. Different weights are assigned to each factor to indicate the importance of its influence on the selection of wells candidates for profile control. Factors have varying values for the selection of wells for profile control.

$$A = (a_i)_{i=1}^n = (a_1, a_2, ..., a_n) \quad (9)$$

In eq 9, a_i is the equivalent weight for each factor ($i = 1, 2,...,n$, n denotes the factor dimension), where A indicates the weight set. The following prerequisites should be met by each factor weight.

$$\sum a_i = 1, \ a_i \geq 0 \quad (10)$$

2.1.3. Creating Evaluation Set. For the evaluation set, the following equations are taken into account.

$$R_i = (r_{ij})_{j=1}^m = (r_{i1}, r_{i2}, ..., r_{im}) \quad (11)$$

In eq 10, r_{ij} is each factor evaluation rate ($i = 1, 2, ..., n$ & $j = 1, 2, ..., m$; here the integers n and m are used. The number of

factors is m, and their dimensions are n). The evaluation matrix is explained in the following equation.

$$R = \begin{bmatrix} R_1 \\ R_2 \\ \vdots \\ R_n \end{bmatrix} = \begin{bmatrix} r_{11} & r_{12} & ... & r_{1m} \\ r_{21} & r_{22} & ... & r_{2m} \\ \vdots & \vdots & \vdots & \vdots \\ r_{n1} & r_{n2} & ... & r_{nm} \end{bmatrix} \quad (12)$$

The comprehensive evaluation set (B) can produce from the multiplication of the factor weight set (A) and the evaluation matrix set (R).

$$B = A \times R = (a_1, a_2, ..., a_n) \cdot \begin{bmatrix} r_{11} & r_{12} & ... & r_{1m} \\ r_{21} & r_{22} & ... & r_{2m} \\ \vdots & \vdots & \vdots & \vdots \\ r_{n1} & r_{n2} & ... & r_{nm} \end{bmatrix} \quad (13)$$

The comprehensive decision-making average value $(\overline{B})$ is obtained by eq 14.

$$\overline{B} = \frac{\sum_{j=1}^m B_j}{m} \quad (14)$$

2.1.4. Application of FEM to the Liuzan Oilfield. As of the end of December 2019, 18 wells in the Liuzan oilfield have valid water injection data for the past 3 years. They are L13-13, L13-21, L15-16, L15-19, L15-21, L15-23, L17-14, L17-23, LB1-4, LB1-8, LB1-12, LB1-14, LB1-15-22, LB1-17-20, LB1-20, LB1-22, LB2-17-11, and LB2-19-13. Vertically, each well has a varied production horizon, ranging from 8 to 78 layers. During production, the production law of each sub-layer is not the same, and the production law of the same sub-layer is relatively close. Therefore, it is necessary to convert the fluid production data of each well according to each sub-layer and finally calculate the profile control. The production data of each well provided on-site contains information such as production time, water injection method, mainline pressure, oil pressure, casing pressure, and daily water injection volume. Each well's geological data included details on the perforations, reservoir physical characteristics, and water absorption profile. After research, it was decided to establish the following indicators to evaluate whether the oil well has profile control requirements.

Water absorption index (K_h) and apparent water absorption index (K_s) can be calculated from water injection data of water well combined with geological data; permeability variation coefficient (K_v) and PI value of water injection well (PI) can be obtained from geological data and the result of the factor value calculation is shown in Table 1. Table 2 shows the factor weight designed for FEM calculation and for each factor it is assumed as 0.25. The process of calculation of well selection decision making for profile control by FEM is illustrated by Figure 1.

2.2. Creation of Factor Weight by RF. By gathering data, developing a model, reducing dimensionality, and improving the predictive model's performance on the issue, scientists can create their predictive modeling project with RF factor weight generation. The RF algorithm used Sci-kit-learn to create the factor weight. When the model is set up, it creates the feature importance (factor weight) property, which determines each feature relative significance scores.

Table 1. Factors for Profile Control Well Selection Based on FEM

no	well ID	K_h	K_s	PI	K_v
1	L13-13	0.303	0.064	0.064	0.056
2	L13-21	0.012	0.099	0.068	0.065
3	L15-16	0.006	0.065	0.057	0.053
4	L15-19	0.009	0.046	0.072	0.053
5	L15-21	0.006	0.040	0.061	0.072
6	L15-23	0.004	0.018	0.057	0.040
7	L17-14	0.017	0.042	0.061	0.053
8	L17-23	0.006	0.080	0.019	0.046
9	LB1-4	0.176	0.042	0.057	0.054
10	LB1-8	0.004	0.010	0.038	0.037
11	LB1-12	0.002	0.015	0.058	0.101
12	LB1-14	0.004	0.090	0.048	0.045
13	LB1-15-22	0.203	0.049	0.057	0.039
14	LB1-17-20	0.026	0.058	0.054	0.090
15	LB1-20	0.026	0.066	0.054	0.041
16	LB1-22	0.031	0.121	0.057	0.055
17	LB2-17-11	0.027	0.061	0.057	0.048
18	LB2-19-13	0.139	0.033	0.058	0.053

Table 2. Factor Weight for FEM

indicators	K_h	K_s	PI	K_v
weight	0.25	0.25	0.25	0.25

$$B = A \times R = \begin{bmatrix} a_{k_h} & a_{k_s} & a_{PI} & a_{k_v} \end{bmatrix} \begin{bmatrix} k_{h1} & k_{h2} & \dots & k_{h18} \\ k_{s1} & k_{s2} & \dots & k_{s18} \\ PI_1 & PI_2 & \dots & PI_{18} \\ k_{v1} & k_{v2} & \dots & k_{v18} \end{bmatrix}$$

$$B = A \times R = \begin{bmatrix} 0.25 & 0.25 & 0.25 & 0.25 \end{bmatrix} \begin{bmatrix} 0.303 & 0.012 & \dots & 0.139 \\ 0.064 & 0.099 & \dots & 0.033 \\ 0.064 & 0.068 & \dots & 0.058 \\ 0.056 & 0.065 & \dots & 0.053 \end{bmatrix}$$

$$B = \begin{bmatrix} 0.122 & 0.061 & 0.045 & 0.045 & \dots\dots & 0.066 & 0.048 & 0.071 \end{bmatrix}$$

Figure 1. Procedure of profile control well selection calculation by FEM.

Table 3 presents the factor weights generated using the RF method for the four factors k_h, k_s, PI, and k_v used for profile

Table 3. Factor Weight Developed by RF

indicators	K_h	K_s	PI	K_v
weight	0.467	0.143	0.197	0.191

control in this study. As observed from Table 3, k_h is the most important factor among the features conducted in this calculation. The process of factor weight generation by the RF algorithm for well selection through FEM proposed by Seddiqi et al.[19] is considered in this section.

3. EXPERIMENTAL STUDY

In this paper, first, the foam system formula, the oil resistance, the temperature resistance, and the salt resistance of the foam system were evaluated by using the waring blender mixing method. The waring blender method is extremely simple and effective in evaluating foam performance. Then, the fractional flow of water was conducted by a flow rate of the foam injection core flood test evaluation. The following material and conditions were considered for all laboratory experiments.

Temperature: formation temperature is 65 °C.
Materials: waring blender, balance (with an accuracy of 0.001 g), temperate box, visualization container, dropper, glass rod, 2000 mL measuring cylinder, and 500 mL beaker.
Foaming agent: sodium dodecyl sulfate (SDS)
Foam stabilizer: hydrolyzed polyacrylamide (HPAM-2500)
Brine: simulate formation water; the degree of salinity is 1572 mg/L.

3.1. Optimal Formulation of Foam Systems. *3.1.1. Experimental Method.* The followings are the steps in the experimental process.

(i) Add a fixed volume of simulated formation water to the beaker;
(ii) Calculate the amount of foaming agent and foam stabilizer, weigh them accurately, add it to the beaker, and stir for about 30 min until it is fully dissolved;
(iii) Evacuate the visualization intermediate container and then inject N_2. The pressure of the container is maintained at 200−300 kPa to ensure that the inside of the container is in an oxygen-free condition;
(iv) Pour the prepared solution into the mixer, stir at high speed until the foam volume is stable, pour it into the intermediate container, and pour it into the visualization container;
(v) Place the foam in a thermostat, observe the change in foam volume over time under anaerobic conditions, and record the half-life.

The stability and foaming ability of the system is evaluated by measuring the half-life and foaming volume of the foam system. During the experiment, each time a fixed volume of 200 mL of foaming liquid was prepared, the volume of foam emitted from it was observed to evaluate the foaming force, and the time required for the volume of foam to decay by half, that is, the half-life of the foam, was recorded.

The foam composite index (FCI) refers to the calculation and evaluation of foam life based on the change in foam volume with time after complete stirring. The relationship between the bubble volume and time is shown in Figure 2.

$$\text{FCI} = S = \int_{t_0}^{t_0 + t_{1/2}} f(t)\mathrm{d}t \tag{15}$$
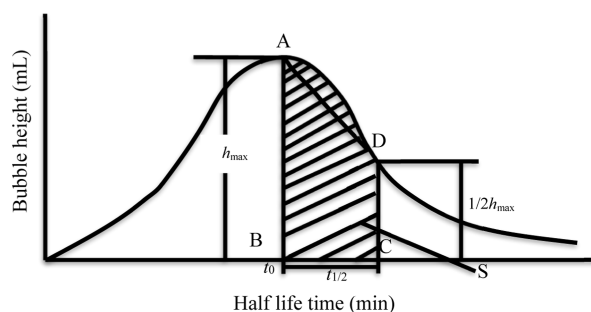
Figure 2. Relationship between bubble height and time.

In eq 15, the FCI is the bubble composite index, min·mL; S is the area of the shaded part is equal to the FCI value; $f(t)$ is the bubble−volume curve; t_0 is the time taken to reach the maximum foaming height or foaming volume, min; and $t_{1/2}$ is the half-life of the foaming liquid, min. For the convenience of calculation, FCI is approximated by the trapezoidal area S.

$$\text{FCI} = S = \int_{t_0}^{t_0+t_{1/2}} f(t)\,\mathrm{d}t = \frac{\left(h_{\max} + \frac{h_{\max}}{2}\right) \times t_{1/2}}{2}$$

$$= 0.75 h_{\max} \times t_{1/2} \tag{16}$$

According to the calculated FCI, the performance of the foam system can be comprehensively evaluated.

3.1.2. Experimental Results and Discussion. Foaming agents (SDS) and foam stabilizers (polymers) are the two key factors in the performance of the foam system. Before optimizing the formulation, it is necessary to evaluate the effects of changes in the amount of SDS and the number of polymers on the foaming ability and stability of the system.

During the experiment, the quantity of polymer was kept constant and the amount of SDS was varied to observe the foaming system. Table 4 shows that with the increase in the

Table 4. Influence of SDS Concentration on the Foam System

SDS (%)	polymer (%)	foaming volume (%)	half-life (min)
0.1	0.3	1550	59
0.2	0.3	1580	57
0.3	0.3	1600	55
0.4	0.3	1650	51

amount of SDS, the foaming volume also increases significantly, while the influence on the half-life of the foam is small. The analysis shows that increasing the amount of SDS can enhance the foaming ability of the system, and has little effect on foam stability. Then, the quantity of SDS was kept constant, and the amount of polymer was varied to observe the quality of the foam system.

Table 5 shows that by increases in polymer concentration the half-life of the foam is significantly prolonged, and the

Table 5. Influence of the Polymer Concentration on the Foam System

SDS (%)	polymer (%)	foaming volume (%)	half-life (min)
0.3	0.1	1500	15
0.3	0.2	1550	40
0.3	0.3	1600	55
0.3	0.4	1650	60

foaming volume does not change significantly. It is concluded that the increase in the amount of polymer can enhance the stability of the foam.

Based on Tables 4 and 5 data, the foam comprehensive index was calculated, and the relationship with the number of chemical agents is shown in Figure 3.

Figure 3 shows that the overall foam performance increases with the increase of SDS and polymer. SDS has little effect on the overall foam coefficient, while the polymer has a greater influence on the foam comprehensive coefficient. Combined with the changing trend of the foam comprehensive index, SDS-0.3% and polymer-0.3% are selected as the optimized foam formula.

3.2. Oil Resistance Evaluation Experiment of Foam System. *3.2.1. Experimental Method.* The simulated formation oil with a viscosity of 1.58 mPa s was used in this experiment. The waring blender stirring method was used to evaluate the oil resistance of the foam system. Specifically, adding different proportions of simulated oil to the foam system. The proportions of simulated oil in the Liuzan oilfield are 0, 15, 25, 35, 45, 55, and 65%, respectively, and the foam system is 0.3% SDS + 0.3% HPAM-2500. The configured oil-containing foam system was diluted to a 200 mL solution, stirred for 5 min with a corrugated mixer at a speed of 8000 rpm, poured it into a 2000 mL graduated cylinder, and the foaming volume (V) and half-life ($t_{1/2}$) were determined and the corresponding FCI was calculated.

3.2.2. Experimental Results and Discussion.

(1) The oil resistance evaluation result of the foam system against the simulated oil in the Liuzan oilfield. The experimental results are shown in Table 6. The oil resistance performance of the foam system under different oil saturation conditions is shown in Figure 4.

Figure 4 shows that as the oil saturation increases, the foaming ability of the foam system decreases. When the oil saturation is greater than 55%, the foaming ability of the system is significantly reduced. As the oil saturation increases, the stability of the foam is enhanced. This is due to the emulsification of the simulated oil and the foam, which makes the foam more stable. Figure 5 shows that although the comprehensive foam index of the system under oily conditions has decreased compared with the foam system under oil-free conditions, the system can maintain a good oil saturation range of less than or equal to 55%. The oil resistance performance of
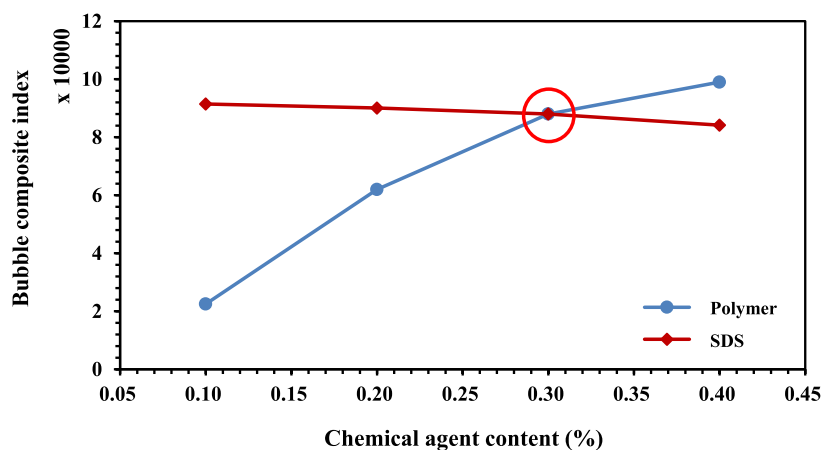
Figure 3. Relationship between SDS and polymer amount and foam comprehensive index.

Table 6. Evaluation Results of the Oil Resistance Performance of the Foam System

no	foam stabilizer	foam stabilizer concentration (%)	foaming agent	foaming agent concentration (%)	oil saturation (%)	foaming volume (mL)	half-life (min)	FCI (mL·min)
1	HPAM-2500	0.3	SDS	0.3	0	1600	55	66,000
2					15	1520	49	55,860
3					25	1450	51	55,462
4					35	1340	52	52,260
5					45	1260	62	58,590
6					55	1150	64	55,200
7					65	850	66	42,075
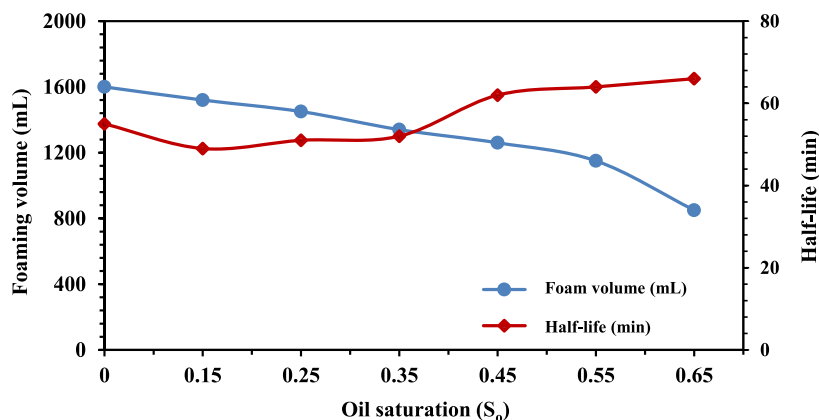
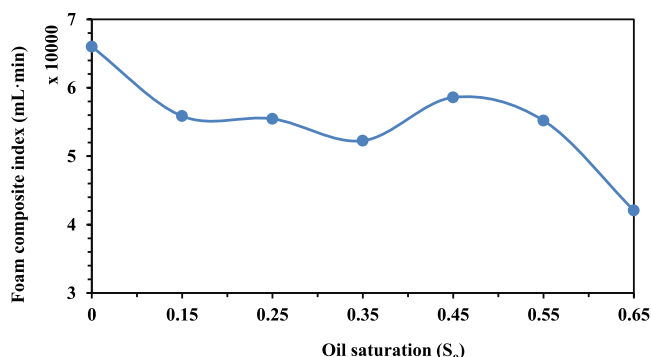**Figure 4.** Comparison of foaming volume and half-life.

Figure 5. Comparison of the FCI.

the system, only when the oil saturation is greater than 55%, the comprehensive foam performance of the system will be significantly reduced. It can be seen that for the crude oil in the Liuzan oilfield, the foam system of 0.3% SDS + 0.3% HPAM-2500 has excellent oil resistance and can maintain good oil resistance within the range of oil saturation less than or equal to 55%.

3.3. Evaluation of the Temperature Resistance of the Foam Systems. *3.3.1. Experimental Method.* The waring blender stirring method was used to evaluate the temperature resistance of the foam system. The simulated temperatures were 60, 85, 100, and 120 °C, respectively. The attenuation of the system was observed in a visual container pre-stored with pure N_2 (200∼300 KPa), as shown in Figure 6. The foam system is 0.3% SDS + 0.3% HPAM-2500. The foam system solution was configured, stirred it for 5 min with a corrugated mixer at a speed of 8000 rpm, poured it into a 3000 mL anaerobic visualization container, and measured the foaming volume and half-life $(t_{1/2})$ of the foam under different temperature conditions and calculated the corresponding FCI.

3.3.2. Experimental Results and Discussion. The experimental results of the foam system under different temperatures are shown in Table 7. The effect of temperature on system performance is shown in Figure 7. Figure 7 shows that as the temperature rises, the stability of the foam system decreases. When the temperature is higher than 100 °C, the stability of the system drops significantly and the foam decay speeds up. It can be seen from Figure 8 that starting from 60 °C, the FCI begins to decrease with the increase in temperature, and it can maintain good stability before 110 °C. When the temperature is greater than 110 °C, the comprehensive foam performance of the system decreases significantly. Comprehensively, the foam system of 0.3% SDS + 0.3% HPAM-2500 has good temperature resistance and can maintain good stability in the temperature range of less than or equal to 110 °C.

3.4. Evaluation of the Salt Resistance in Foam Systems. *3.4.1. Experimental Method.* The waring blender stirring method was used to evaluate the salt resistance of the foam system. The formation water with salinities of 8000, 20,000, 30,000, 40,000, and 50,000 mg/L and the foam system of 0.3% SDS + 0.3% HPAM-2500 were used to configure the foaming system. The configured foam system was diluted to a 200 mL solution, stirred for 5 min with a corrugated mixer at a speed of 8000 rpm, and poured it into a 2000 mL graduated cylinder to determine the foam volume and it is the half-life $(t_{1/2})$ under different formation water salinity conditions and calculated the corresponding FCI.

3.4.2. Experimental Results and Discussion. Table 8 shows the evaluation results of the salt resistance performance of the foam system. The salt tolerance of the foam system under different salinity conditions is shown in Table 8.

It can be seen from Figures 9 and 10 that, relative to the initial salinity of 1572 mg/L, with the increase of the salinity of the formation water, the foaming ability and half-life of the
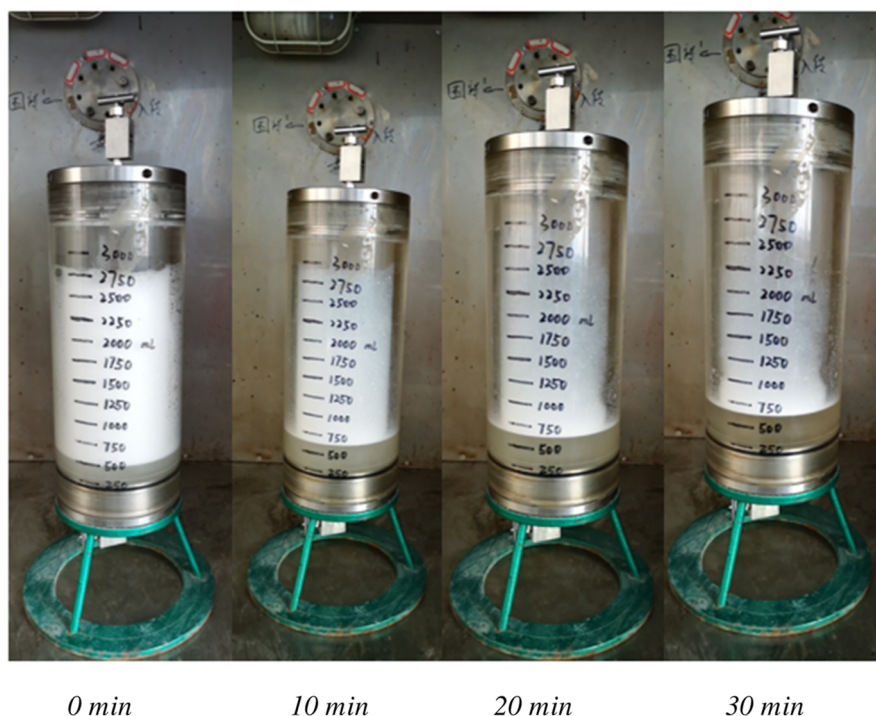
0 min   *10 min*   *20 min*   *30 min*

Figure 6. Experimental process of the foam temperature resistance performance under the condition of 95 °C pure N_2.

Table 7. Evaluation Results of the Temperature Resistance Performance of the Foam System

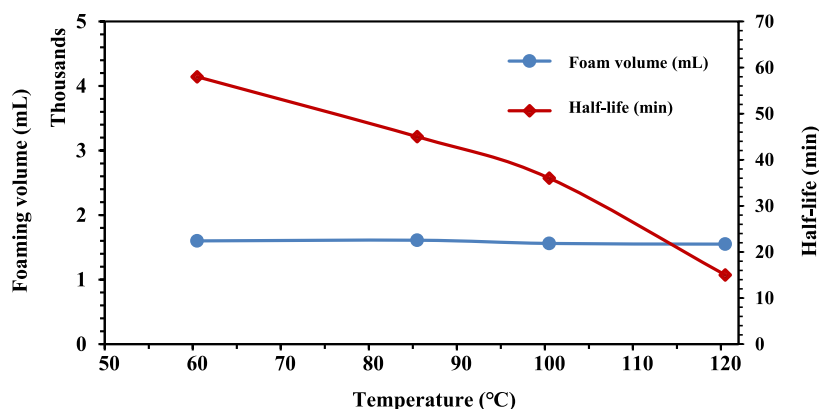| no	foam stabilizer	foam stabilizer concentration (%)	foaming agent	foaming agent concentration (%)	temperature (°C)	foaming volume (mL)	half-life (min)	FCI (mL·min)
1	HPAM-2500	0.3	SDS	0.3	60	1600	58	69,600
2					85	1610	45	54,337
3					100	1560	36	42,120
4					120	1550	15	17,437

Figure 7. Comparison of foaming volume and half-life.

foam system decreases, and the degree of salinity of formation water has a greater impact on foam stability. When the formation water salinity is greater than 40,000 mg/L, the foaming capacity, half-life, and FCI of the foam will decrease sharply. The foam system of 0.3% SDS + 0.3% HPAM-2500 has excellent salt tolerance and can maintain good salt tolerance within the range of formation water salinity less than or equal to 40,000 mg/L.

3.5. Evaluation of the Flow Rate of the Foam System.

3.5.1. Experimental Conditions. Foaming agent: 0.3% SDS

Polymer: 0.3% HPAM-2500

Brine: simulated formation water with a salinity of 1572 mg/L.

Core: manually suppress a 30 × 4.5 × 4.5 cm heterogeneous model.

Temperature: the simulated formation temperature was 95 °C.

The experimental equipment mainly included a 2PB00C series advection pump from the Beijing satellite manufacturing plant, a core holder, a pressure sensor, and a thermostat.

3.5.2. Experimental Methods. The artificially compressed heterogeneous core model is used to select different
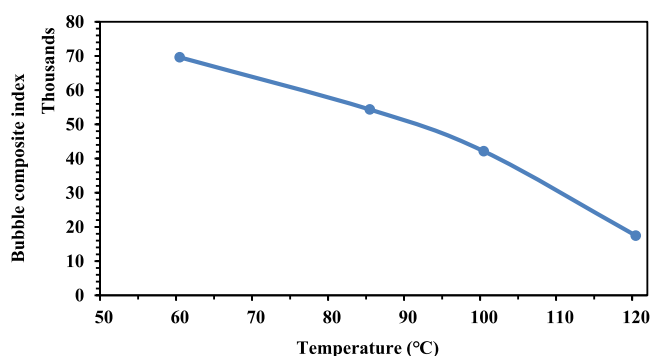
Figure 8. Comparison of the FCI.

permeability differences (50−500 mD) to determine the shunt rate of the foam system under the conditions of different permeability differences. The experimental steps were as follows.

(i) Simulate the formation conditions of the Jidong oilfield, artificially suppress the heterogeneous model, a core length of 30 cm, a width and height of 4.5 cm, and the total core volume calculated.

(ii) Put the compressed core into the holder, add clean water to a confining pressure of 3 MPa with a hand pump, and vacuum the model for 5 h to saturate the simulated formation water, record the saturated volume, calculate the porosity, and measure the permeability with water flooding.

(iii) Put the saturated heterogeneous core model in a constant temperature box for 12 h, then adopt the mode of combined injection and separate extraction, and inject the simulated formation water at an injection rate of 0.5 mL/min. The injection rate is 1 PV, and the exit of the high permeability section is recorded. Calculate the flow rate of the liquid output separately from the outlet of the low-permeability section.

(iv) Inject the gas−liquid slugs at an injection rate of 0.5 mL/min, keep the gas−liquid slug ratio at 1:1, and each time the gas−liquid alternate injection volume is 0.05 PV, and record the liquid output during the injection of the foam system, calculate the shunt rate.

(v) Conduct secondary water flooding at an injection rate of 0.5 mL/min, and stop the flooding when the shunt rate is restored before the controlled flooding.

3.5.3. Experimental Results and Discussion. The experimentally suppressed heterogeneous core model, using the form of co-injection and separate mining, was used to observe the profile control effect of the foam system using a 50−500 mD heterogeneous core at 95 °C. The experimentally determined shunt rate is shown in the figure. Under the condition of 95 °C, it can be seen from Figure 11 that the flow

rate of high permeability and low permeability is obvious in the first water flooding stage. After the foam system was injected, the difference between high- and low-permeability cores was significantly improved, the fluid production of high permeability decreased, and the split flow of low permeability increased correspondingly, indicating that the foam system played a better profile control effect, and the profile improvement rate reached more than 95%. In the secondary water flooding stage, the diversion rate of low permeability can reach as high as 59.9%, and that of high permeability is 40.1%. The results show that after profile control of the foam system, the high-permeability channeling flow can be effectively controlled, the low-permeability water flooding is continuously enhanced, and the system has a better control and flooding effect.

4. SIMULATION STUDY

4.1. Numerical Inversion of Integral Plugging Adjustment in a Three-Dimensional Model of Multi-Layer Sandstone. The Computer Modeling Group, CMG-STARS numerical simulation software, is used to simulate the equivalent three-dimensional experimental model; the size of the plane grid is 30 × 4.5 × 4.5 cm (equivalent three-dimensional model), designed the same as the experimental heterogeneous model and illustrated in Figure 12. A total of four simulation layers are divided longitudinally, the thickness of a single layer is 1.25 cm, and the thickness of the model is 4.5 cm.

The model has two different permeability layers 50 and 500 mD. Two injection wells were considered for injecting foam parameters and N_2 at the start of the model. Two production wells were considered at the end of the model to produce the liquid from different permeability layers.

When the permeability is 50 mD, the experimental value agrees well with the fitted values, as shown in Figure 12. According to the multi-layer sandstone physical simulation experiment process, the specific experimental steps of setting the numerical inversion are as follows.

Well-Inj injected water at a rate of 0.5 mL/min, and well-inj copy, injected gas N_2 with the same quantity of polymer and surfactant injected. As mentioned above, well-pro (high-permeability) and well-pro (low-permeability) are used for water production from high and low permeability layers, respectively.

Experiments and numerical simulations were carried out on a modified foam system. As shown in Figure 13, when 0.1 PV modified foam is injected, the experimental value is 0.1% at 50 mD and 0.9% at 500 mD, and when the foam is injected, it changes to 0.35 and 0.65%, respectively. Compared to the experiment, it is the closest to the test result. Based on the simulation result, it is possible to apply the foam flooding

Table 8. Test Results of the Salt Resistance Evaluation of the Foam System

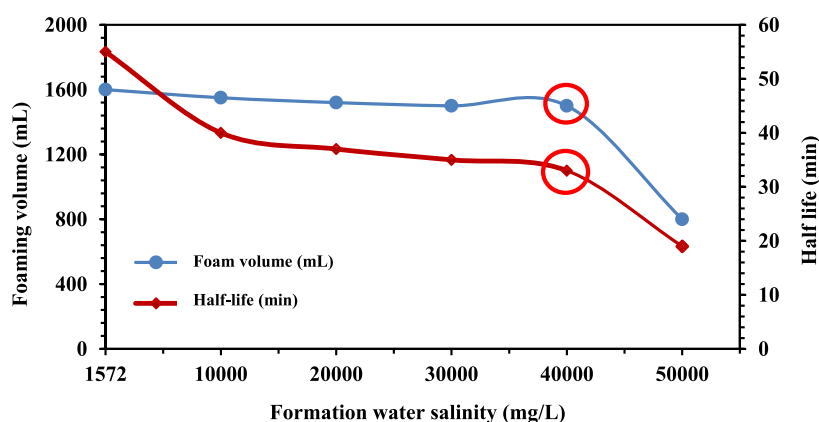| no	foam stabilizer	foam stabilizer concentration (%)	foaming agent	foaming agent concentration (%)	formation water salinity (mg/L)	foaming volume (mL)	half-life (min)	FCI (mL·min)
1	HPAM-2500	0.3	SDS	0.3	1572	1600	55	66,000
2					8000	1550	40	46,500
3					20,000	1520	37	42,180
4					30,000	1500	35	39,375
5					40,000	1500	33	37,125
6					50,000	800	19	11,400

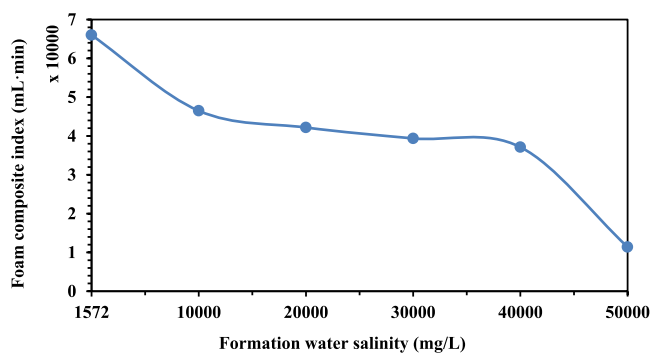**Figure 9.** Comparison of foaming volume and half-life.

Figure 10. Comparison of foam system performance under different salinities.

experiment to the designated oilfield and the foam details could be the same as the core model simulation.

4.2. Numerical Simulation of Liuzan Oilfield.
4.2.1. Geological Model Establishment and Parameter Preparation. The Liuzan oilfield is an important development sector of the Jidong oilfield; it was discovered in 1990 and has been steadily developing since then. It has been involved in various stages of investigation and development during the past 2 decades. The oil reservoir in the block covers an extent of around 50 km. The simulated area of the block contains 124 wells. The grid should be separated into parallel or orthogonal directions according to the oilfield structure principle. It should also have a clear boundary and a fault line. The grid's direction also links to the reservoir properties. It can either be parallel or perpendicular to the fluid's flow direction. The size and location of the grid are also consistent with well positions.

The grid is divided using the method of separating the layers along the x and y axes, with a 100 meter step between each point. The vertical direction is separated into 30 tiny layers based on the idea that the permeability difference between the layers should not exceed 3. The microstructure map of tiny sand body thicknesses in the rhythm section of the Liuzan block is utilized to control the tectonic fluctuation of the layers. In the simulation model, the total grid is considered $30 \times 60 \times 30 = 54,000$.

4.2.2. Influence of Profile Control. In the present simulation study, the HPAM-2500 and SDS foam system were used as a profile control plugging agent. The foam system condition was designed the same as the experimental core flood numerical simulation model developed in Section 4.1. Initially, the simulation of the foam plugging profile control system is applied to the selected wells by the FEM. The oil recovery by foam plugging profile control system was calculated. Then, the method is applied to the wells selected by the factor weight developed by the RF, and both methods' results are compared.

In the simulation model, the foam was injected for 3 days into the wells selected for profile control. The polymer, surfactant, and water are injected into the selected wells to make foam. The same selected wells are copied and used for the N$_2$ injection at the same time when the foam is injected. The foam system profile controlled the seven wells chosen by FEM and the four wells chosen by the factor weight developed by the RF model. The mole fractions of the injected
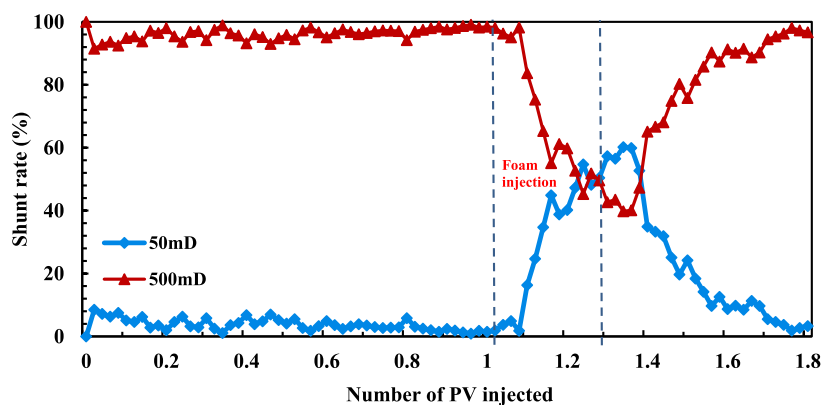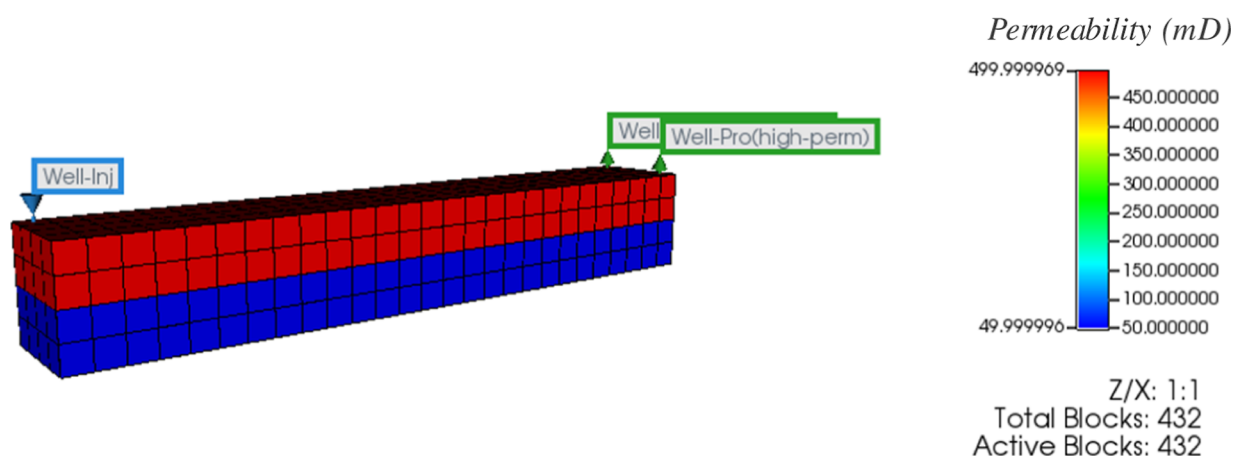

Figure 11. System flow rate curve at 95 °C.

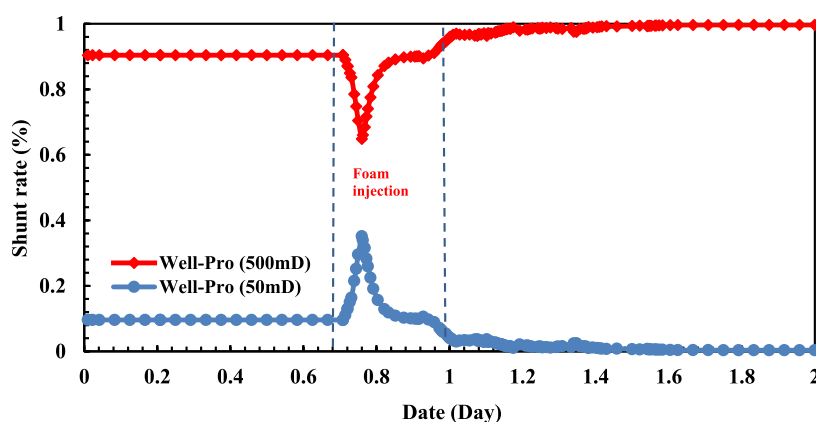**Figure 12.** Multi-layer sandstone equivalent numerical model.

Figure 13. Influence of foam injection on the flow shunt of water in a simulation model built based on a laboratory test.

components of water, polymer, and surfactant are 0.999730922, 5.43113e-006, and 0.000263647, respectively. The injection surface liquid and gas rate of 50 m³/day has been considered.

5. RESULTS AND DISCUSSION

5.1. FEM Result. The comprehensive decision-making average value ($\overline{B}$) is calculated by FEM and shown in Figure 14, which is equal to $\overline{B} = 0.055$. Those wells are considered for profile control which the average value ($\overline{B}$) is larger than the comprehensive evaluation value (B). Figure 14 shows that 7 wells, wells L13-13, L13-21, LB1-4, LB1-15-22, LB1-17-20, LB1-22, and LB2-19-13 of the 18 candidate wells were selected, while wells L15-16, L15-19, L15-21, L15-23, L17-14,

L17-23, LB1-8, LB1-12, LB1-14, LB1-20, and LB2-17-11 have not been selected for profile control.

5.2. RF Result. Table 9 shows the profile control well selection results using the factor weight developed by the RF method. By this method, 4 wells, L13-13, LB1-4, LB1-15-22,

Table 9. Profile Control Well Selection Result by Using the Factor Weight Developed by RF

| no	well ID	B	$\overline{B}$	result
1	L13-13	0.174	0.055	selected
2	L13-21	0.046		not selected
3	L15-16	0.033		not selected
4	L15-19	0.035		not selected
5	L15-21	0.034		not selected
6	L15-23	0.023		not selected
7	L17-14	0.036		not selected
8	L17-23	0.026		not selected
9	LB1-4	0.110		selected
10	LB1-8	0.017		not selected
11	LB1-12	0.034		not selected
12	LB1-14	0.032		not selected
13	LB1-15-22	0.120		selected
14	LB1-17-20	0.048		not selected
15	LB1-20	0.040		not selected
16	LB1-22	0.053		not selected
17	LB2-17-11	0.041		not selected
18	LB2-19-13	0.091		selected
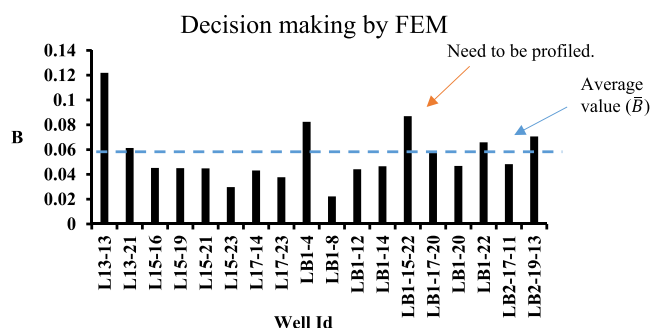
Figure 14. Profile control well selection results by FEM.

and LB2-19-13, out of 18 candidate wells are chosen for profile control.

5.3. Numerical Simulation Result. To evaluate the efficiency of profile control in Liuzan oilfield through the foam system plugging agent in the selected wells by the FEM and RF models parameters such as the effective period length, oil increment, water reduction, average oil increment, and daily water reduction and cumulative oil production during the 5 years after the foam injection which is assumed as effective period have been compared. The component mole fraction used in this numerical simulation study is denoted in Table 10.

Table 10. Injection Fluid Component Mole Fraction

components	mole fraction
water	0.999881402
surfactant	5.43195×10^{-6}
polymer	0.000113166
total	1

The time span known as the effective period refers to the interval between turning on the producer and the water cut recovering to the point where the foam was not injected. The number of days that foam treatment causes a decrease in water production is the effective period.

Based on simulation model results, the foam system profile control applied to the four wells selected by the RF compared to the base and FEM models has a better result in terms of the oil production increased during the effective period. The case with seven wells chosen by FEM has a substantially better efficiency in increasing the oil production during the long term.

A decreasing value is observed in the water cut of both FEM and RF models after the foam system profile control is applied. Getting back to the value of the water cut before applying the foam system profile control takes a longer time.

In the profile control results for the wells chosen by FEM, the value of the water cut is higher compared to the factor weight developed by the RF model, and 1800 days are considered the effective period. The two methods' well selection for profile controls the FEM, and RF in terms of daily oil production rate, cumulative oil production rate, and water cut are compared in Figure 15. Considering the average value of daily water reduction and oil increase during the effective period, the good results are from RF well selection model. The average values represent the efficacy of the effects of foam injection. Table 11 shows the cumulative, daily oil production average value, and the water cut average value of the base, FEM, and RF models.

In FEM, the factor weight can be calculated using a variety of approaches. The entropy approach, the criterion importance method, the analytic hierarchy process, and the inter-criteria correlation are a few examples.[21−29] The entropy weight is compared to the results of the FEM and RF approaches in this research. Zheng and Tian presented the entropy approach for determining the factor weight in 2009.[20] It accomplishes this by estimating the amount of information available in a given system.

The procedure described in this paper is compared to the entropy method weight computation. The weight is calculated using the entropy approach on the same set of data as the FEM. The K_h, K_s, PI, and K_v weight values are calculated to be 0.22, 0.23, 0.42, and 0.13 respectively. The entropy technique produces the same well selection results as the FEM, but it
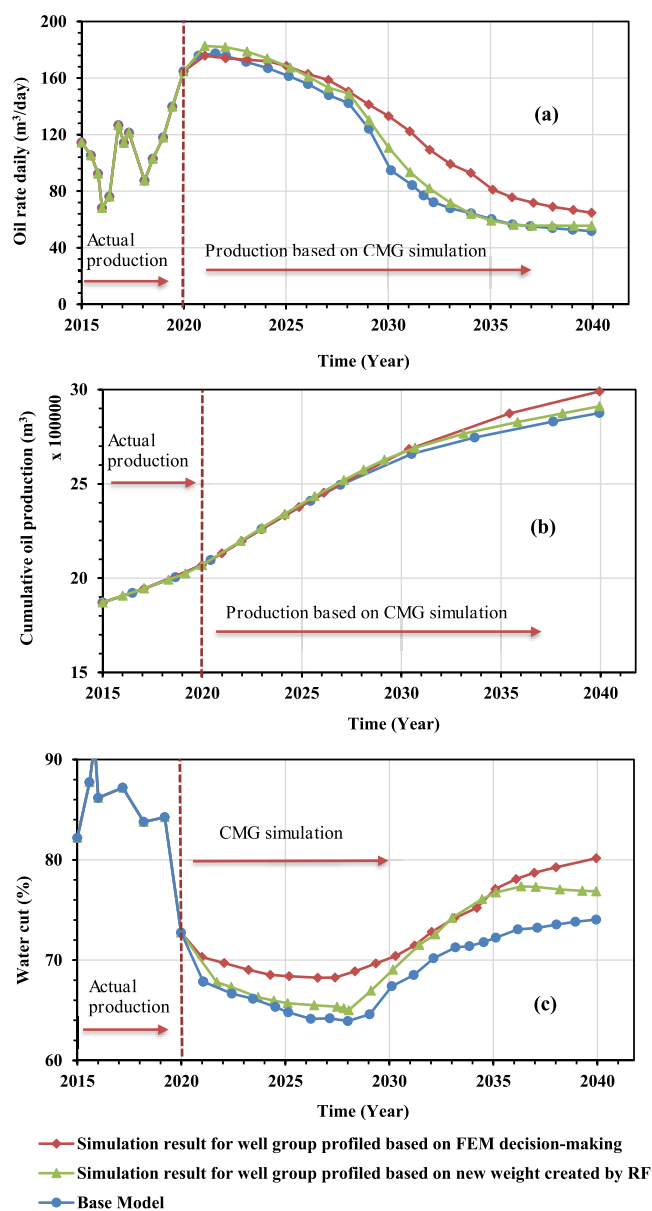
Figure 15. Foam plugging influence on (a) daily oil production rate, (b) cumulative oil production rate, and (c) water cut of the Liuzan oilfield for wells are chosen for profile control by FEM, the factor weight developed by RF and base models (in the base model, no wells selected for profile control and foam is not injected in it).

differs significantly from the RF method. Expanding the data and calculating the factor weight using production history is relatively simple with the RF approach. Unfortunately, classic factor weight computation methods remain inefficient and time-consuming. This research applied a new approach of well selection for profile control established using the RF algorithm on an actual oilfield, which is more favorable and simple to use.

6. CONCLUSIONS

The FEM is conducted for well-selection decision-making for profile control in the field of development engineering. Since the factor weight is considered subjectively, the decision-making by this method is inaccurate, as a result, the development of FEM by proposing an accurate factor weight study is urgently necessary. In this paper, the RF algorithm is used to calculate the factor weight. The factors used for profile

Table 11. Influence of Foam Injection Profile Control Result of the Two Models FEM and RF, and Comparing Them with the Base Model During the Effective Period

model	cumulative oil production (m³) 1/1/2020 -1/1/2025	oil rate daily (m³/day) production average 1/1/2020-1/1/2025	water cut SC-% average 1/1/2020 -1/1/2025
base model	2,380,119	171.58	67.419
wells selected by FEM	2,381,773	172.52	70.515
wells selected by using new factor weight	2,391,584	177.91	68.296

control can differ depending on the availability of the data. The factor weights generated by RF were used in the FEM and new well selection data for profile control have been suggested. Following the implementation of the well group profile control by foam system, the oilfield reduced water and boosted oil output, while the nearby oil wells had noticeable effects. The cumulative oil increases after profile control of the wells selected by FEM and using the factor weight developed by RF are 1654 and 11,465 m³ during the effective period, respectively. The following are the major conclusions drawn from this paper:

(1) The FEM was applied in the Liuzan oilfield to select candidate wells for profile control, and as a result, seven wells were selected for the foam plugging system;

(2) Based on this study, the four wells were selected for profile control by using the factor weight developed by RF;

(3) The foam system profile control is analyzed in a laboratory foam flood experimental test. In the experiment, the formula of the foam system, oil resistance, temperature resistance, salt resistance, and flow rate of the foam system was evaluated. As a result, the foam system was confirmed as a better profile control agent and a 95% improvement blocking succeeded;

(4) The foam system experimental test model was simulated by CMG-STARS to get the possibility of applying the profile control on a designated oilfield;

(5) The profile controlled by a foam system on the Liuzan oilfield wells selected by FEM, factor weight developed by RF, and the base model was applied and compared.

■ AUTHOR INFORMATION

Corresponding Authors

Khwaja Naweed Seddiqi − *China University of Petroleum-Beijing, The Unconventional Oil and Gas Institute, Beijing 102249, China; Graduate School of International Resource Sciences, Department of Earth Resource Engineering and Environmental Science, Akita University, Akita 010-8502, Japan;* orcid.org/0000-0003-3871-6445; Email: naweed.cedeqe@gmail.com

Hongda Hao − *School of Petroleum Engineering, Changzhou University, Jiangsu 213164, China;* Email: haohongda90@126.com

Jirui Hou − *China University of Petroleum-Beijing, The Unconventional Oil and Gas Institute, Beijing 102249, China;* Email: houjirui@126.com

Authors

Kazunori Abe − *Graduate School of International Resource Sciences, Department of Earth Resource Engineering and Environmental Science, Akita University, Akita 010-8502, Japan;* orcid.org/0000-0001-9781-2416

Zabihullah Mahdi − *Graduate School of International Resource Sciences, Department of Earth Resource Engineering and Environmental Science, Akita University, Akita 010-8502, Japan*

Huaizhu Liu − *China National Petroleum Corporation, Drilling & Production Technology Research Institute, Jidong Oilfeld Company, CNPC, Tangshan 063000 Hebei, China*

Complete contact information is available at:
https://pubs.acs.org/10.1021/acsomega.2c08002

■ REFERENCES

(1) Khojastehmehr, M.; Madani, M.; Daryasafar, A. Screening of enhanced oil recovery techniques for Iranian oil reservoirs using TOPSIS algorithm. *Energy Rep.* **2019**, *5*, 529−544.

(2) Höök, M.; Hirsch, R.; Aleklett, K. Giant oilfield decline rates and their influence on world oil production. *Energy Pol.* **2009**, *37*, 2262−2272.

(3) Höök, M.; Xu, T.; Xiongqi, P.; Aleklett, K. Development journey and outlook of Chinese giant oilfields. *Petrol. Explor. Dev.* **2010**, *37*, 237−249.

(4) Song, W.; Yang, C.; Han, D.; Qu, Z.; Wang, B.; Jia, W. Alkaline-surfactant-polymer combination flooding for improving recovery of the oil with high acid value. In *International Meeting on Petroleum Engineering*; OnePetro, 1995.

(5) Grigg, R. B.; Schechter, D. S. State of the Industry in CO2 Floods. *SPE Annual Technical Conference and Exhibition*; OnePetro, 1997.

(6) Xia, T.; Feng, Q.-h.; Wang, S.; Zhang, X.-m.; Ma, Z.-y. Decision-Making Technology of Well Candidates Selection in In-depth Profile Control Based on Projection Pursuit Clustering Model. *International Field Exploration and Development Conference*; Springer, 2019; pp 1737−1751.

(7) Su, Y.; Li, Y.; Wang, L.; He, Y. Experimental and pilot tests of deep profile control by injecting small slug-size nano-microsphere in offshore oilfields. In *Offshore Technology Conference*; OnePetro, 2019.

(8) Qiu, Y.; Wei, M.; Bai, B.; Mao, C. Data analysis and application guidelines for the microgel field applications. *Fuel* **2017**, *210*, 557−568.

(9) Qiu, Y.; Wei, M.; Bai, B. Descriptive statistical analysis for the PPG field applications in China: Screening guidelines, design considerations, and performances. *J. Petrol. Sci. Eng.* **2017**, *153*, 1−11.

(10) Feng, Q.; Chen, Y. Application of fuzzy mathematics to block-wide injection profile control. *Petrol. Explor. Dev.* **1998**, *25*, 76−79.

(11) Liu, Y.; Bai, B.; Li, Y.; Coste, J. P.; Guo, X. Optimization design for conformance control based on profile modification treatments of multiple injectors in a reservoir. In *International Oil and Gas Conference and Exhibition in China*; OnePetro, 2000.

(12) Jiang, H. Q.; Wang, S. L.; Zhang, Y. Pre-warning and decision making of water breakthrough for higher water-cut oilfield. In

Advanced Materials Research; Trans Tech Publications, 2012; pp 688–693.

(13) Li, X. Application of Fuzzy Mathematics Evaluation Method in Prediction of Comprehensive Efficiency of Low Efficiency Oil Wells. In *IOP Conference Series: Earth and Environmental Science*; IOP Publishing, 2019; Vol. *384*, p 012012.

(14) Zhang, X.; Li, Q.; Li, X. The application of fuzzy mathematics in the optimization of oilfield development scheme. *NW. Geol.* **2002**, *1*, 76–80.

(15) Tang, H.; Huang, B.; Li, D. Fuzzy comprehensive evaluation method to determine the potential of reservoir water flooding development. *Pet. Explor. Dev.* **2002**, *2*, 97–99.

(16) Li, Y. Pressure Index Decision Technology for Integrated Profile Control in a Block. *J. Univ. Pet.* **1997**, *21*, 39–42.

(17) Qin, G.; Pan, P.; Tao, H. The analysis and application of PI decision making technology. *Neimenggu Shiyou Huagong* **2005**, *8*, 120–123.

(18) Liu, Y.; Bai, B.; Wang, Y. Applied technologies and prospects of conformance control treatments in China. *Oil Gas Sci. Technol.* **2010**, *65*, 859–878.

(19) Seddiqi, K. N.; Hao, H.; Liu, H.; Hou, J. Decision-Making Techniques for Water Shutoff Using Random Forests and Its Application in High Water Cut Reservoirs. *ACS Omega* **2021**, *6*, 34327–34338.

(20) Zheng, W.; Tian, Q. The application of entropy method and AHP in weight determining. *Comput. Program. Skills Maint.* **2009**, *22*, 19–20.

(21) Liu, L.; Zhou, J.; An, X.; Zhang, Y.; Yang, L. Using fuzzy theory and information entropy for water quality assessment in Three Gorges region, China. *Expert Syst. Appl.* **2010**, *37*, 2517–2521.

(22) Zhang, P.; Feng, G. Application of fuzzy comprehensive evaluation to evaluate the effect of water flooding development. *J. Pet. Explor. Prod. Technol.* **2018**, *8*, 1455–1463.

(23) Amiri, V.; Rezaei, M.; Sohrabi, N. Groundwater quality assessment using entropy weighted water quality index (EWQI) in Lenjanat, Iran. *Environ. Earth Sci.* **2014**, *72*, 3479–3490.

(24) Hsu, L.-C. Using a decision-making process to evaluate efficiency and operating performance for listed semiconductor companies. *Technol. Econ. Dev. Econ.* **2015**, *21*, 301–331.

(25) Zhang, H.-P. Application on the entropy method for determination of weight of evaluating index in fuzzy mathematics for wine quality assessment. *Adv. J. Food Sci. Technol.* **2015**, *7*, 195–198.

(26) Şahin, M. A comprehensive analysis of weighting and multicriteria methods in the context of sustainable energy. *Int. J. Environ. Sci. Technol.* **2021**, *18*, 1591–1616.

(27) Xu, M. L.; Zhao, D. S. Application of Entropy-Weight Hierarchy Analysis on Study of Height Prediction of Water Conducted Zone. In *Advanced Materials Research*; Trans Tech Publications, 2013; Vol. *742*, pp 497–500.

(28) Zhu, Y.; Tian, D.; Yan, F. Effectiveness of entropy weight method in decision-making. *Math. Probl Eng.* **2020**, *2020*, 3564835.

(29) Aomar, R. A. *A Combined ahp-Entropy Method for Deriving Subjective and Objective Criteria Weights*; SSRG, 2010.